

Study on effects of mudsill and infilled wallboard on response of steel frame under curvature surface deformation

Wei Xie^{1,2,3}, Junwu Xia^{1,a}, Yuying Zheng², Qiufen Wang², Hongfei Chang¹ and Shangtong Yang⁴

¹School of Mechanics and Civil Engineering, China University of Mining and Technology, 221116 Xuzhou, China

²Xuhai College, China University of Mining and Technology, 221008 Xuzhou China

³Jiangsu Collaborative Innovation Center for Building Energy Saving and Construction Technology, Jiangsu Vocational Institute of Architectural Technology, 221116 Xuzhou, China

⁴Department of Civil and Environmental Engineering, University of Strathclyde, G1 1XJ Glasgow, United Kingdom

^aCorresponding author: xjunw@163.com

Abstract. The structural performance of steel frames with novel lightweight composite infilled wallboard is experimentally and numerically investigated under the curvature surface deformation. This study compares the mechanical behavior for the open-frame, the closed-frame with mudsill and the closed-frame with infilled wallboard, through experiment and finite element analysis, under the positive and negative curvature surface deformations respectively. The structural responses such as basement counterforce, additional strains at different key locations and the effects of mudsill and infilled wallboard are evaluated. It has been found that the steel frames with the new composite infilled wallboard can considerably increase the stiffness of the structures in resisting surface deformation and re-distribute the loads amongst the beam and column members in the frame. The force transmission effect of the mudsill accelerated the changes in the additional strain at column bottom. Frame beam is the main component that bears the curvature surface deformation. Mudsill has a consistent stress pattern with the frame beam and can significantly influence additional strain of the frame beam due to its stress sharing effect. The infilled wallboard is connected with the column-beam members and thereby influences the additional strain of the frame column significantly.

1. Introduction

Surface deformation is a common consequence of undersurface activities, e.g., mining, water table change, tunneling, crustal movement [1-3]. The surface deformation can cause damage to the structures above the ground due to the imbalanced supporting from the foundation. However, it is still not very much clear with regard to the understanding of the structural performance of the steel frame buildings with infill walls which are subjected to surface deformation. It results in major challenge in the design and safety assessment of these structures.

In the context of increasing industrial applications of buildings in surface deformation regions, a number of studies on the surface deformation resistance of structures have been reported [4-7].



Meanwhile, the wall component plays an important role in the structural frame performance and thus has attracted considerable research interest. The steel frame infilled with different types of wall (such as masonry wall, autoclaved cellular concrete (ACC) wall, polymer matrix composite (PMC) wallboard) were investigated and the studies on the influences of infilled walls on frame performance mainly concentrated on the lateral stiffness and the seismic behavior of the structure [8-17].

There are very limited researches in investigating the surface deformation resistance of the structures and perhaps none in incorporating the honeycomb autoclaved lightweight concrete (ALC) composite infilled walls. This paper attempts to carry out both experiment and finite element analysis (FEA) for a number of steel frames with/without mudsill and infilled walls under positive and negative curvature surface deformations.

2. Experimental design and FEA model

The structure researched is a typical single-layer two-span steel frame. The steel Q235 is used (one type of steel in China with the yielding strength $f_y=235\text{Mpa}$). The beam-column sections adopt the H-shape. The honeycomb sandwich wallboard has a total thickness of 100mm and combined 2 outer-panels which are made of autoclaved lightweight concrete (ALC). The honeycomb core board is manufactured into the honeycomb-shape by paper material. The curvature surface deformation was loaded through the displacement-control method. The base of column B was fixed and the bases of columns A and C were descended (positive curvature surface deformation loading) or ascended (negative curvature surface deformation loading) by jacks. The diagrammatic sketch of experimental apparatus is shown in Figure 1.

The FEA model corresponding to the physical experiment was established. The beam and column adopted 2-node 3D finite strain linear beam element with 6 DOF for each node, and bilinear isotropic hardening model was used for the properties of steel material of the frame. The infill wallboards were placed and connected into the steel frame through the clamp-plate and bolt-plate on the beam and column. From the force transmission perspective, this wallboard-frame connection mode is the rigid point connection. According to the characteristic of wallboard-frame connection mode, the rigid connecting area is small and arranged in a discrete distribution. Therefore, the wallboard-frame connection was achieved or modeled as follows: the edge of wallboard outer-panel element coincided with the inner flange of the beam or column element; 3 translational DOF (U_x , U_y , U_z) of the node of beam or column element and the node of the wallboard outer-panel element were kept in accordance by the way of node coupling in the connection areas as shown in Figure 2. 4-node 6 DOF elastic shell element was used to simulate the ALC outer-panel, and 2-node 3D spring-damper elements arranged between elastic shell elements were used to simulate the honeycomb core board, as shown in Figure 2. For the infilled wallboard, the elastic modulus E of the ALC panel and the axial spring stiffness K of spring-damper element were determined by in-plane and out-plane compression tests of honeycomb sandwich wallboard, respectively.

3 types of frames were made in terms of the placement of mudsill and/or infilled wallboard, i.e., open frame (no mudsill and no infilled wallboard), closed frame (with mudsill but no infilled wallboard) and frame with infilled wallboard (with mudsill), which are identified separately as OPfr, CLfr, WAfr in experiment and FE-OPfr, FE-CLfr, FE-WAfr in FEA.

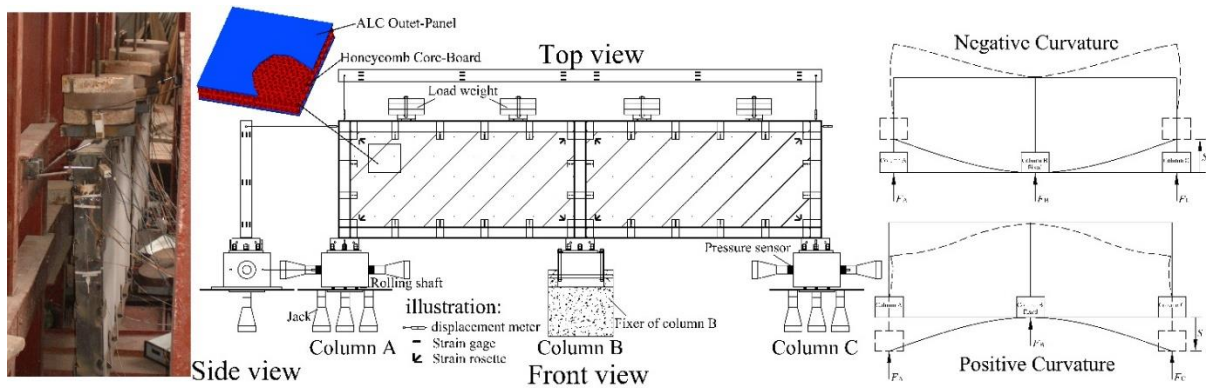


Figure 1. Diagrammatic sketch of experimental apparatus of curvature surface deformation

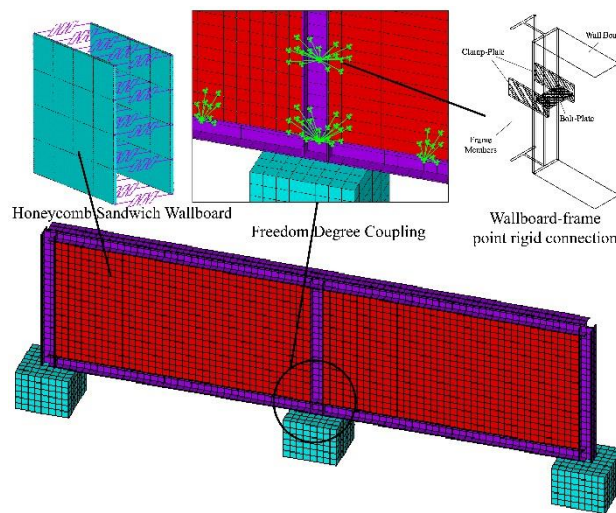
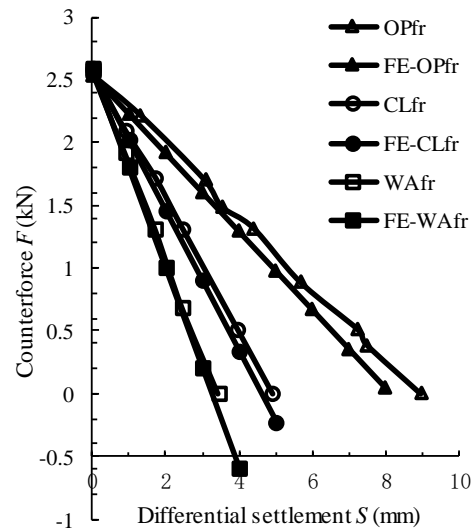


Figure 2. FEA model for experiment (frame with infill wall as an example)

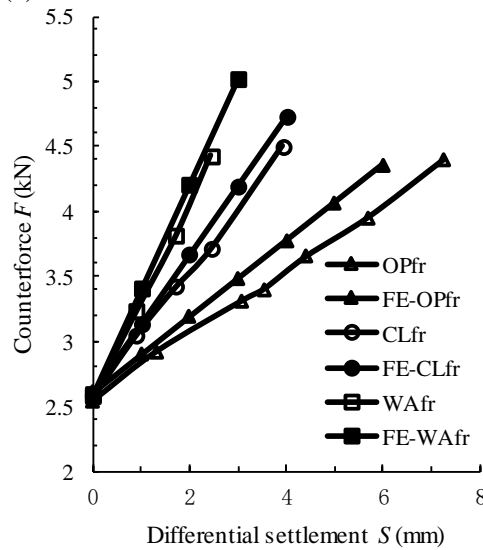
3. Comparison of experiment and FEA

3.1 Basement counterforce analysis

The 3 types of frames (i.e., open frame, closed frame and closed frame with infilled wallboard) have different rigidities, which cause different basement counterforce variations at every displacement variation level. The curvature surface deformations are compared in terms of the counterforce at the basement of the side columns (F). The variation law obtained from the experiment and FEA of F with S are shown in Figure 3.



(a) Positive curvature surface deformation



(b) Negative curvature surface deformation

Figure 3. Relation curves of differential settlement- counterforce of side columns

The differential settlement of the basement counterforce of the side columns in the 3 types of frames presents a linear variation with the curvature surface deformation. The variation rates of basement counterforce between 3 types of frames are shown in Figure 4 (positive curvature surface deformation abbreviated as PCD, negative curvature surface deformation abbreviated as NCD).

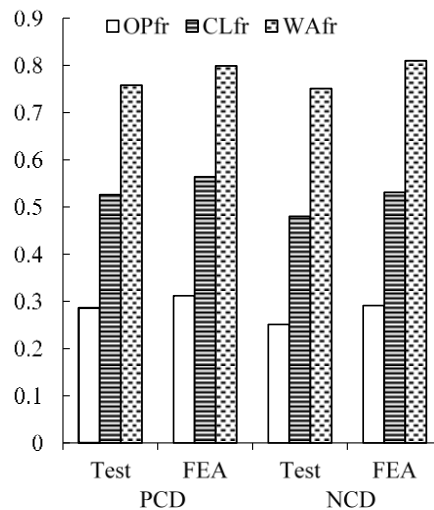


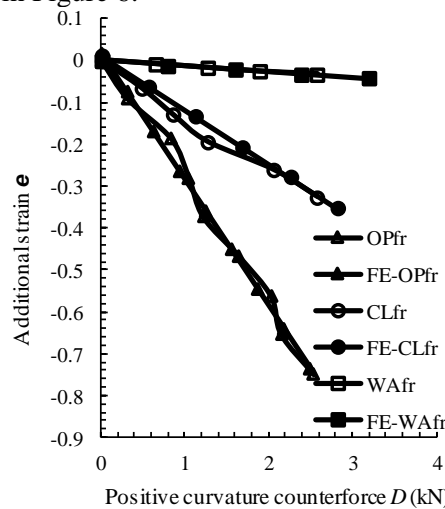
Figure 4. Comparison of variation rates of counterforce between frames

Apparently, under the same displacement loading rate, the WAfr shows the maximum variation rate of basement counterforce of the columns, followed by the CLfr and then the OPfr. In other words, under the same displacement increment, the variation of basement counterforce is positively correlated with the stiffness of the frame.

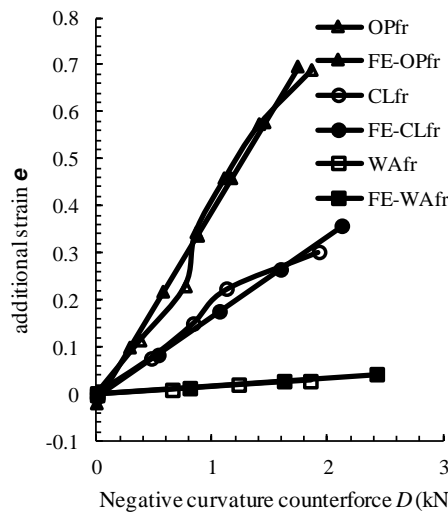
For the sake of convenience, a relative force parameter D is introduced which represents the difference between the basement counterforce and the initial counterforce ($D = |F - F_0|$). D presents a proportional relationship with S ($D = kS$, where k is the absolute value of the slope of the $F-S$ linear function). D reflects the curvature surface deformation by the basement counterforce, which can also be called the curvature counterforce.

3.2 Additional strain analysis of columns

The variation laws of additional strain at outer flange of side column top in the 3 types of frames under curvature counterforce obtained by FEA and experiment are shown in Figure 5 which shows that the strains at the same position at the outer flange of the side column are opposite in sign under the positive and negative curvature counterforces. Both strains present a linear growth with the curvature counterforce. The variation rate of additional strain at the outer flange of the side columns top between the 3 types of frames are shown in Figure 6.



(a) Positive curvature surface deformation



(b) Negative curvature surface deformation

Figure 5. Relation curves of counterforce-additional strain at outer flange of side columns top

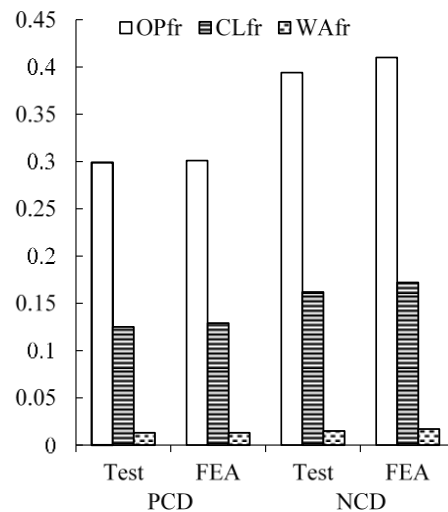
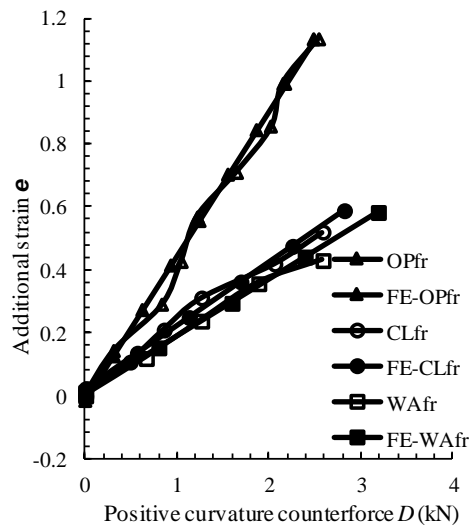


Figure 6. Comparison of variation rates of additional strain at outer flange of side column top

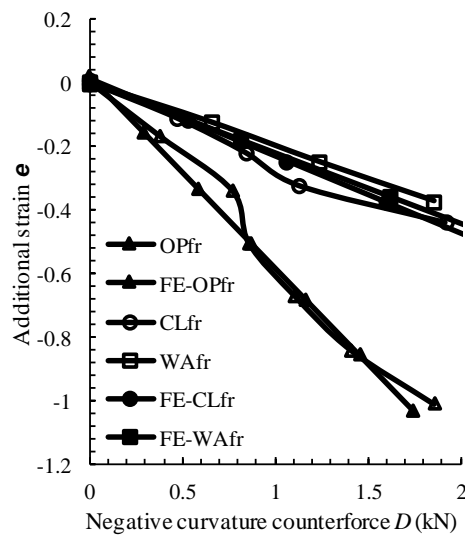
Both the mudsill and infilled wallboard decelerates the variation of additional strain on the side column top. By contrast, the effect of infilled wallboard to the variation-rate of additional strain at outer flange of side columns top is greater than that of the mudsill.

3.3 Additional strain analysis of frame beam

The variation laws of additional strain at the upper flange of middle-column-end of frame beams in 3 types of frames with curvature counterforces obtained by FEA and experiment are shown in Figure 7. The additional strains of the beams under the positive and negative curvature surface deformations are opposite and present a linear growth with the curvature counterforce. The comparison of the variation rates of the additional strain at the frame beams among the 3 types of frames are shown in Figure 8.



(a) Positive curvature surface deformation



(b) Negative curvature surface deformation

Figure 7. Relation curves of counterforce-additional strain at upper flange of middle-column-end of frame beam

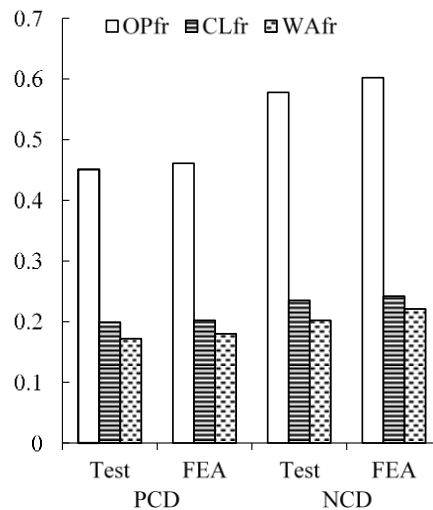


Figure 8. Comparison of variation rates of additional strain at upper flange of middle-column-end of frame beam

Both mudsill and infilled wallboard decelerate the variation of additional strain at the beam ends under curvature deformations. Mudsill decreases the variation rate of additional strain at the beam ends more significantly than infilled wallboard.

4. Conclusions

On the basis of the comprehensive contrast analysis of the variation of the structural responses of the 3 types of frames under positive and negative curvature surface deformations, the following conclusions are obtained:

(1) The differential settlement and basement counterforce of frame are significantly affected by the frame stiffness. The arrangement of mudsill and infilled wallboard increases the stiffness of the frame significantly, thus accelerating the variation of the basement counterforce and decreasing the final differential settlement.

(2) The curvature surface deformation experiment is easy to control and operate by the displacement loading method, but because of the different stiffness of the upper structures, the change rate of the basement counterforce can be different, and then there will be interference to the contrast study between different stiffness structures. According to the variation law of the basement counterforce with the settlement difference of curvature surface deformation, the curvature reaction counterforce is introduced to represent the curvature surface deformation instead of the curvature settlement difference, which is used as the unified contrast parameter of the different stiffness structures under the displacement loading condition. The variation rate of basement counterforce is avoided from interfering with the contrast analysis.

(3) The FEA models of 3 types of steel frames, which can well reflect the physical experiment, are established. The spring damper elements arranged between shell elements, and the relevant parameters seted based on the wallboard test well simulated the performance of the honeycomb sandwich wallboard. The connection area nodes between frame elements and wallboard shell elements are coupled to restrict the translational DOF, which effectively simulates the rigid point-type connection between beam/column and wallboard.

(4) By comparison, the effect of the mudsill is more significant on additional strain of frame beam and that of the wallboard is more significant on additional strain of column. It is because under the curvature surface deformation, columns, which are the force transmission components, transmit the basement counterforce to the beam and the beam is the main component that bears the curvature surface deformation. As a horizontal component parallel to the beam, the stress pattern of mudsill is consistent

with the frame beam, and mudsill mainly shares stress and deformation from the beam. In particular, because the bottom of the column is the connecting part with mudsill, the force transfer effect of mudsill increases the variation rate of additional stress in this part.

(5) As a plane component that connects beam and column, the wallboard take part in the work to a large extent. The infilled wallboard mainly combines frame components into an integral system and increases the internal stress distribution among beams and columns, thus influencing the additional strain of the frame columns significantly.

Acknowledgements

This work was financially supported by the National Science Foundation of China (Grant No. 51274192, 51408596), the Jiangsu Province Science Foundation of China (Grant No. BK20140195), the Natural Science Foundation of the JiangSu Higher Education Institutions of China (Grant No. 16KJB560021), the Qing Lan Project of Jiangsu Colleges and Universities of China, the Open Foundation of Jiangsu Collaborative Innovation Center for Building Energy Saving and Construction Technology Open Foundation of China (Grant No. SJXTQ1617).

References

- [1] D.L. Galloway, D.R. Jones, S.E. Ingebritsen, *Land subsidence in the United States*. (U.S. Geological Survey Circular, 1999)
- [2] H. Bouwer, *Ground Water*, **15**, 5 (2010)
- [3] A. Klein, W. Jacoby, P. Smilde, *Earth Planet. Sc. Lett.*, **147** (1997)
- [4] R.C. Speck, R.W. Bruhn, *Environ. Eng. Geosci.*, **1**, 1 (1995)
- [5] O. Deck, M.A. Heib, F. Homand, *Eng. Struct.*, **25**, 4 (2003)
- [6] D.F. Laefer, S. Ceribasi, J.H. Long, et al., *J. Geotech. Geoenviron.*, **135**, 11 (2009)
- [7] W. Xie, J.W. Xia, Y.Y. Zheng, *J. of SiChuan Univ.: Eng. Sci. Ed.*, **47**, 2 (2015)
- [8] T. Suzuki, H. Choi, Y. Sanada, et al., *B Earthq. Eng.*, **15**, 10 (2017)
- [9] P.G. Asteris, L. Cavaleri, F.D. Trapani, et al., *Eng. Struct.*, **132** (2017)
- [10] G. De Matteis, *J. Earthq. Eng.*, **4**, 3 (2000)
- [11] A.J. Aref, W.Y. Jung, *J. Struct. Eng.-ASCE*, **129**, 4 (2003)
- [12] D.M. Carradine, F.E. Woeste, J.D. Dolan, et al., *Forest Prod. J.*, **54**, 5 (2004)
- [13] S.H. Basha, H.B. Kaushik, *Eng. Struct.*, **111** (2016)
- [14] L. Cavaleri, M. Papia, *Eng. Struct.*, **25** (2003)
- [15] A. Mohebkah, A.A. Tasnimi, H.A. Moghaddam, *J. Constr. Steel. Res.*, **64**, 12 (2008)
- [16] H.A. Moghadam, M.G. Mohammadi, M. Ghaemian, *J. Constr. Steel. Res.*, **62** (2006)
- [17] K.M. Amanat, E. Hoque, *Eng. Struct.*, **28** (2006)